Dynamics of a disordered monatomic solid with continuous distribution of force constants

Andrzej Czachor
Institute of Physics, Polish Academy of Sciences, Warsaw, Poland
(Received 12 November 1985)

The average local-information transfer approximation (ALITA) Green's function $\langle \vec{\vec{G}}_{\mathbf{Q}}(\omega)\rangle$ (where $\mathbf{Q}$ and ω are the wave vector and the frequency, respectively) and related longitudinal (L) and transverse (T) dispersion curves, frequency spectrum and neutron inelastic scattering (NIS) cross section have been calculated for a monatomic solid, disordered with respect to interatomic coupling and atomic configuration. Rectangular, elliptic, and Lorentz distributions of the self-force constants in the nearest-neighbor central-force model have been assumed. It has been found that the frequency spectrum of such a system is dominated by a huge peak at the average Einstein frequency due to the T curve, and a bump at lower frequency representing the first minimum in the L curve. Force disorder manifests itself in extending the range of frequencies and in rounding off the details of the spectrum corresponding to configuration disorder. Besides, the plane-wave deformations with wave vectors in certain "Q gaps" cannot contribute to normal modes of vibration in disordered solids. The NIS cross section at large momentum transfer $\hbar\mathbf{Q}$ leads directly to the spectrum of Einstein frequencies. If this spectrum has a sharp edge at 0, then essential deviations from the Debye type of frequency spectrum and from the T^3 law for vibrational specific heat at low temperatures do appear.

I. INTRODUCTION

Numerical investigation of large clusters of topologically disordered atomic systems leads to a good description of the experimental situation for several disordered solids—see, e.g., the review of Hafner.[1] However, due to the finite dimensions of such clusters (less than ten atoms in one direction), some arbitrariness in taking boundary conditions, and several approximate, although ingenious, tricks in the numerical procedure, the quality of the description does not necessarily mean that all has been explained. In particular, the numerical procedures are not very useful in predicting correlations between experimental spectra. To do that one has to have a simple (even if approximate) and transparent approach. Such an approach has been recently developed—an analytic construction of various spectra in terms of the same Green's function for topologically disordered solids.[2,3] Let us briefly recall the idea.

For monoatomic systems the frequency spectrum can be expressed exactly, and the neutron inelastic scattering (NIS), the first-order Raman (FOR), and the infrared absorption (IRA) spectra can be expressed approximately in terms of the Fourier transform of the displacement-displacement Green's function

$$\langle \vec{\vec{G}}_{\mathbf{Q}}(\omega)\rangle = \int dt\, e^{i\omega t}\frac{1}{N}\sum_{\mathbf{R},\mathbf{R}'}\langle\langle \mathbf{u}_{\mathbf{R}}(t),\mathbf{u}_{\mathbf{R}'}(0)\rangle\rangle e^{i\mathbf{Q}\cdot(\mathbf{R}-\mathbf{R}')}\,, \tag{1}$$

where $\mathbf{u}_{\mathbf{R}}(t)$ is the displacement at time t of an atom from its average position $\mathbf{R}$. For example, the (squared) frequency spectrum is ($\lambda\sim\omega^2$),

$$G(\lambda)\sim\sum_{\mathbf{Q}}\mathrm{Im}[\mathrm{Tr}\langle \vec{\vec{G}}_{\mathbf{Q}}(\omega+i\varepsilon)\rangle]\,, \tag{2}$$

i.e., the frequency spectrum is $g(\omega)=2\omega G(\omega)$, whereas the NIS cross section has roughly the form

$$\frac{d^2\sigma^{\mathrm{NIS}}}{d\omega\, d\Omega}\sim n(\omega)\mathbf{Q}\cdot\mathbf{Q}(-\mathrm{Im}\langle \vec{\vec{G}}_{\mathbf{Q}}(\omega+i\varepsilon)\rangle)\,, \tag{3}$$

where $\hbar\mathbf{Q}$ and $\hbar\omega$ are momentum and energy transfers in the scattering, respectively, and $n(\omega)$ is the Bose-Einstein factor. Similar expressions appear in the FOR and IRA cases.

The function $\langle \vec{\vec{G}}_{\mathbf{Q}}(\omega)\rangle$, central to this approach, has been derived in the average local-information transfer approximation (ALITA) and applied to model-disordered solids with isotropic and central forces between nearest neighbors. With use of this function, the impact of configuration disorder, mass disorder, and force disorder corresponding to two different scalar self-force matrices has been established.[2,3]

In this work we intend to determine in full the role of disorder in interatomic coupling, using the above-mentioned nearest-neighbor central-force model.[2] It should be emphasized that such interatomic forces are in general capable of securing the stability of solids. Such a model was recently used also by Bhatia and Singh to fit the "phonon dispersion curves," found numerically by several authors.[4] We assume the force-constant matrix (of the theory of small variations) between the atom at the average position $\mathbf{R}$ and its nearest neighbor at $\mathbf{R}'=\mathbf{R}+\mathbf{W}_{\mathbf{R}}$ to be (see Fig. 1)

$$\vec{\vec{\Phi}}_{\mathbf{R},\mathbf{R}'}=\vec{\vec{\Phi}}_{\mathbf{R},\mathbf{W}_{\mathbf{R}}}=\begin{cases}-l\hat{\mathbf{W}}_{\mathbf{R}}\hat{\mathbf{W}}_{\mathbf{R}} & \text{for } |\mathbf{W}_{\mathbf{R}}|=W\,,\\ 0 & \text{otherwise,}\end{cases} \tag{4}$$

where $\hat{\mathbf{W}}=\mathbf{W}/W$, the W is the distance between nearest neighbors, and l is a coupling parameter. With the num-

ber of interacting nearest neighbors n and the parameters l and W fixed, and possible differences in the self-force matrices for different atoms

$$\overleftrightarrow{\Psi}_{\mathbf{R}}=-\sum_{\mathbf{W_R}}\overleftrightarrow{\Phi}_{\mathbf{R},\mathbf{W_R}} \tag{5}$$

neglected [Eq. (5) is in fact the translational invariance condition], we have arrived in Ref. 3 at the following "dispersion curves," corresponding to purely configurational disorder

$$\begin{aligned}\Omega_{\mathrm{L}}^2&=\frac{2nl}{M}h_2(QW)\,,\\ \Omega_{\mathrm{T}}^2&=\frac{nl}{M}[h_0(QW)-h_2(QW)]\,,\end{aligned} \tag{6}$$

where, with $p=QW$

$$\begin{aligned}h_0(p)&=\frac{1}{2}\left[1-\frac{\sin p}{p}\right],\\ h_2(p)&=\frac{1}{6}\left[1+6\frac{\sin p-p\cos p}{p^3}-3\frac{\sin p}{p}\right].\end{aligned} \tag{7}$$

Both curves correspond to the poles of the ALITA Green's function $\langle\overleftrightarrow{G}_{\mathbf{Q}}(\omega)\rangle$. At the same time the curve Ω_{L} is the predicted geometric place of the NIS-peak positions in the ω-Q plane. In this case there is no force disorder.

What happens if there are a number of different coupling parameters, assigned at random to interatomic bonds? The answer[2,3] turns out to depend on self-forces: If there is a finite number of different self-force matrices then there appears a comparable number of frequency gaps in the frequency spectrum and in the dispersion curves of such a system. For example, with two self-force matrices corresponding to isotropic coupling, $\Psi_A\overleftrightarrow{1}$ and $\Psi_B\overleftrightarrow{1}$, in concentrations $c_A+c_B=1$, we have single gap near the average Einstein frequency $[(c_A\Psi_A+c_B\Psi_B)/M]^{1/2}$. Some of these gaps have been observed in the NIS spectra for substitutional alloys,[5-7] but not for topologically disordered solids so far.

In this paper we assume an extended distribution of force constants, continuous in a certain range. Physically it may be due to a continuous distribution of the interatomic distances or to interbond angles varying in a continuous way throughout the solid. Apparently, the normal-mode patterns of atomic displacements should be more peculiar here than in the former cases. It will be shown below, however, that even in this case there are interesting manifestations of coherence in the NIS spectra, as far as the ALITA scheme may be relied upon.

In Sec. II we introduce the distributions and derive the Green's function. Dispersion curves are discussed in Sec. III. To calculate the frequency spectrum we have to introduce the cutoff function to carry out the Q integration in Eq. (2), as discussed in Sec. IV. The possibility of determining the distribution of Einstein frequencies from experimental data is discussed in Sec. V. In Sec. VI we examine the plane-wave contribution of normal modes in disordered systems. Finally, in Sec. VII we try to support the idea that known anomalies in frequency spectra and specific heat of disordered systems may be due to a singular pileup of Einstein frequencies in the zero-frequency limit. Conclusions are given in Sec. VIII.

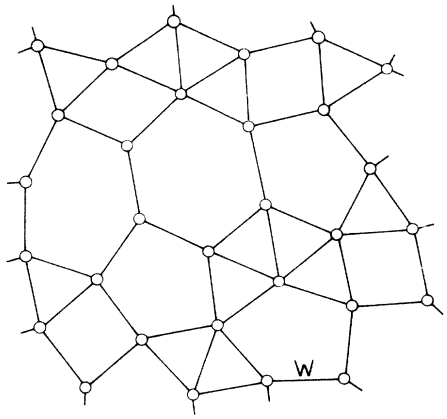

FIG. 1. Model of monatomic disordered structure with the nearest-neighbor bond distance W fixed. Central-force model arises if the interatomic bonds are free springs.

II. CALCULATION OF THE GREEN'S FUNCTION $\langle\overleftrightarrow{G}_{\mathbf{Q}}(\omega)\rangle$

We have to establish the form of the Green's function $\langle\overleftrightarrow{G}_{\mathbf{Q}}(\omega)\rangle$ and of the related functions assuming such distributions of force constants, which make the task both reasonable and tractable. Let us start from some of the general formulas of Refs. 2 and 3. In the ALITA one finds the following form of the Green's function for a monatomic solid:

$$\begin{aligned}\langle\overleftrightarrow{G}_{\mathbf{Q}}(\omega)\rangle&=\frac{\hat{\mathbf{Q}}\hat{\mathbf{Q}}}{\omega^2M-\Phi_Q^{\mathrm{L}}(\omega)}+\frac{\overleftrightarrow{1}-\hat{\mathbf{Q}}\hat{\mathbf{Q}}}{\omega^2M-\Phi_Q^{\mathrm{T}}(\omega)}\\ &\equiv\hat{\mathbf{Q}}\hat{\mathbf{Q}}\Gamma_Q^{\mathrm{L}}+(\overleftrightarrow{1}-\hat{\mathbf{Q}}\hat{\mathbf{Q}})\Gamma_Q^{\mathrm{T}}\,,\end{aligned} \tag{8}$$

where $\hat{\mathbf{Q}}=\mathbf{Q}/Q$, and the form of the $\mathbf{Q}$ dependence follows from isotropy of the system; M stands for atomic mass. The functions $\Phi_Q^{\mathrm{L,T}}(\omega)$ are related to the effective dynamical matrix

$$\overleftrightarrow{\Phi}_{\mathbf{Q}}^{\mathrm{eff}}=\frac{\langle(\overleftrightarrow{\mathrm{L}\Phi})_{\mathbf{Q}}\rangle}{\langle L\rangle}=\hat{\mathbf{Q}}\hat{\mathbf{Q}}\Phi_Q^{\mathrm{L}}(\omega)+(\overleftrightarrow{1}-\hat{\mathbf{Q}}\hat{\mathbf{Q}})\Phi_Q^{\mathrm{T}}(\omega)\,, \tag{9}$$

where

$$\langle(\overleftrightarrow{\mathrm{L}\Phi})_{\mathbf{Q}}\rangle=\frac{-2}{N}\sum_{\mathbf{R},\mathbf{R}'}\overleftrightarrow{\mathrm{L}}_{\mathbf{R}}\overleftrightarrow{\Phi}_{\mathbf{RR}'}\sin^2[\mathbf{Q}\cdot(\mathbf{R}-\mathbf{R}')/2] \tag{10}$$

and $\langle L\rangle$ is the average locator:

$$\langle L\rangle=1/3N\sum_{\mathbf{R}}\mathrm{Tr}\overleftrightarrow{\mathrm{L}}_{\mathbf{R}}\,,$$

where the locator is

$$\overleftrightarrow{\mathrm{L}}_{\mathbf{R}}=(\omega^2M\overleftrightarrow{1}-\overleftrightarrow{\Psi}_{\mathbf{R}})^{-1}\,. \tag{11}$$

TABLE I. Components of dimensionless locator $\Lambda(\lambda)$.

Distribution	$\rho(\lambda)=\Lambda_2(\lambda)/\pi$ $(x=\lambda-1)$	$\Lambda_1(\lambda)$ $(x=\lambda-1)$
rectangular	$\frac{1}{2a}\Theta(a^2-x^2)$	$\frac{1}{2a}\ln\left\|\frac{a+x}{a-x}\right\|$
elliptical	$\frac{2}{\pi a^2}\Theta(a^2-x^2)(a^2-x^2)^{1/2}$	$\frac{2}{a^2}[x-(\mathrm{sgn}x)\Theta(x^2-a^2)(x^2-a^2)^{1/2}]$
Lorentzian	$\frac{1}{\pi}\frac{a}{a^2+x^2}$	$\frac{x}{a^2+x^2}$

Now we shall apply the above to the system of atoms interacting with the forces given by (4), i.e., only the coupling between the atoms at the distance W is different from zero. As W is fixed, the formula (10) factorizes into the product of the Q-dependent and the ω-dependent terms, which is a crucial simplification. Previously we obtained the functions Φ_Q^L, Φ_Q^T in Ref. 3:

$$\Phi_Q^L(\omega)=2A(\omega)h_2(p)\,,$$
$$\Phi_Q^T(\omega)=A(\omega)[h_0(p)-h_2(p)]\,, \tag{12}$$

where $A(\omega)$ is the frequency-dependent effective constant between nearest neighbors. To establish its form let us take the trace of the matrix (9) and average it over the solid angle. The result is

$$A(\omega)=3(M\omega^2-1/\langle L\rangle)\,. \tag{13}$$

As $A(\omega)$ depends, through $\overleftrightarrow{L}_R$, only on the self-force matrix $\overleftrightarrow{\Psi}_R$ and on ω, we can say that within this model the problem of force disorder reduces to the problem of the self-force disorder (diagonal disorder). The coupling parameter l in Eq. (4) and, therefore, the self-force matrix (5), are free to assume any values.

Now the only thing to do is to calculate the average locator $\langle L\rangle$. Let the eigenvalues of the matrices $\overleftrightarrow{\Psi}_R$ be $\Psi_{R,\nu}$, $\nu=1,2,3$. We assume the distribution of all eigenvalues Ψ to be extended, continuous in a certain range, and centered at a certain value Ψ_0; we shall call it the distribution of self-forces, equivalently we may speak of the distribution of (squared) Einstein frequencies $\omega_{R,\nu}^2=\Psi_{R,\nu}/M$. The range mentioned above will be called here the band of force disorder. Using these notions we can introduce the dimensionless locator $\Lambda(\lambda)$:

$$\langle L(\omega+i\varepsilon)\rangle=\frac{1}{3N}\sum_{R,\nu}\frac{1}{M(\omega+i\varepsilon)^2-\Psi_{R,\nu}}$$
$$=\frac{1}{\Psi_0}\left[\mathrm{P}\int_0^\infty\frac{\rho(\lambda')}{\lambda-\lambda'}d\lambda'-i\,\mathrm{sgn}(\varepsilon\omega)\pi\rho(\lambda)\right]$$
$$\equiv\frac{1}{\Psi_0}[\Lambda_1(\lambda)-i\,\mathrm{sgn}(\varepsilon\omega)\Lambda_2(\lambda)]\,, \tag{14}$$

where $\rho(\lambda)$ is the distribution of the eigenvalues in the units $\omega_0^2=\Psi_0/M$, normalized to unity, and $\lambda=(\omega/\omega_0)^2$.

We shall consider in some detail the three model self-force distributions given in Table I and displayed in Fig.

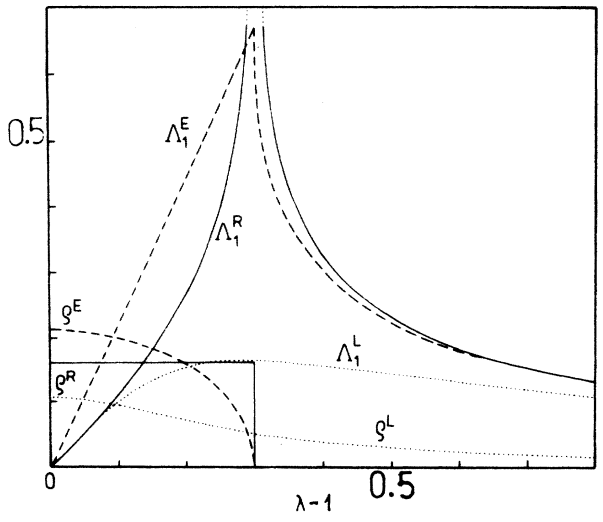

FIG. 2. Elliptic (E), rectangular (R), and Lorentzian (L) distributions of self-force constants $\rho(\lambda)$ and corresponding real parts of a dimensionless locator $\Lambda_1(\lambda)$, see Table I. Width parameter $a=0.3$.

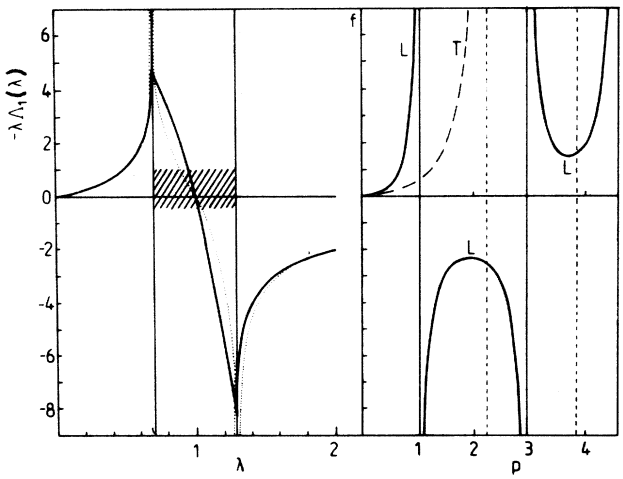

FIG. 3. Plot of both terms of Eq. (19) for $a=0.3$. Left-hand side: thick and dotted lines correspond to elliptic and rectangular distributions, respectively. Right-hand side: functions $f_p^{L,T}$ as given by Eq. (16). Vertical scale is the same in both pictures. Dashed vertical lines are asymptotes of the f_p^T, which is out of scale except for $p<2$.

2. They are symmetric with respect to $\lambda=1$. This means that Ψ_0 is the average self-force constant and ω_0 is the average Einstein frequency. The width parameter a is a measure of the interatomic coupling disorder. From now on we assume $\omega>0$, i.e., $\mathrm{sgn}(\varepsilon\omega)=1$ and we can forget it. The functions Γ^{L} and Γ^{T} of Eq. (8) can now be written as follows ($p=QW$):

$$\Gamma_p^{\mathrm{L,T}}(\omega)=\frac{1}{\Psi_0}i_p^{\mathrm{L,T}}f_p^{\mathrm{L,T}}\frac{\Lambda(\lambda)}{\lambda\Lambda(\lambda)+f_p^{\mathrm{L,T}}}\ , \tag{15}$$

where

$$f_p^{\mathrm{L,T}}=(i_p^{\mathrm{L,T}}-1)^{-1},\quad i_p^{\mathrm{L}}=[6h_2(p)]^{-1}\ ,$$

$$i_p^{\mathrm{T}}=[3h_0(p)-3h_2(p)]^{-1}\ . \tag{16}$$

Functions $f_p^{\mathrm{L,T}}$ are displayed in Fig. 3. Now we have to distinguish between two cases:

(i) $\rho(\lambda)\neq 0$, i.e., the frequency is in the band of disorder; it is so for $1-a<\lambda<1+a$ for rectangular and for elliptic distribution. One obtains from (15):

$$-\mathrm{Im}\Gamma^{\mathrm{L}}(\omega+i\varepsilon)=\frac{i_p(f_p^{\mathrm{L}})^2}{\Psi_0\lambda}\frac{\pi\lambda\rho(\lambda)}{[f_p^{\mathrm{L}}+\lambda\Lambda_1(\lambda)]^2+[\pi\lambda\rho(\lambda)]^2}\ . \tag{17}$$

(ii) $\rho(\lambda)=0$, i.e., the frequency is outside the range of the self-force distribution, e.g., $1-a>\lambda$ or $\lambda>1+a$ for rectangular or for elliptic distribution; shortly, we are out of the band of disorder. Formally we can take the limit $[\pi\lambda\rho(\lambda)]\to 0$ in (17) to arrive at

$$-\mathrm{Im}\Gamma_Q^{\mathrm{L}}(\omega+i\varepsilon)=\frac{i_p^{\mathrm{L}}(f_p^{\mathrm{L}})^2}{\Psi_0\lambda}\pi\delta(f_p^{\mathrm{L}}+\lambda\Lambda_1(\lambda))\ . \tag{18}$$

Let us remember that the function $-\mathrm{Im}\Gamma^{\mathrm{L}}(\omega+i\varepsilon)$ gives the NIS profile (3). In the band of disorder the $-\mathrm{Im}\Gamma^{\mathrm{L,T}}(\omega+i\varepsilon)$ profiles are broad. Obviously it is so everywhere with the Lorentz distribution, see Fig. 4. However, as the peak width $\sim\lambda\rho(\lambda)/|\Lambda_1(\lambda)|$, it goes to zero for $\lambda\to 0$ (acoustic limit) even in this case.

III. DISPERSION CURVES

Now let us look at the "dispersion curves" given by the equation

$$\Delta^{\mathrm{L,T}}(\lambda)\equiv\lambda\Lambda_1(\lambda)+f_p^{\mathrm{L,T}}=0\ . \tag{19}$$

These equations may have many solutions for a given Q—see Fig. 3. The Q ranges, where they have the out-of-band solutions

$$-\mathrm{Im}\Gamma^{\mathrm{L,T}}(\omega+i\varepsilon)\sim I_p^{\mathrm{L,T}}\delta(\lambda-\lambda_p^{\mathrm{L,T}})\ , \tag{20}$$

[where λ_p are the roots of (19) and $I_p=1/|\Delta'(\lambda_p)|$], will be called the coherence ranges. The NIS profiles are δ functions there. The remaining Q ranges, those without solutions, will be called the Q gaps. Figure 5 shows the plot of the dispersion curve λ_p^{L} and its intensity I_p^{L} versus p, for elliptic distribution.

It is clear from Fig. 2 that with rectangular distribution the sequence of the coherence ranges is infinite—see the

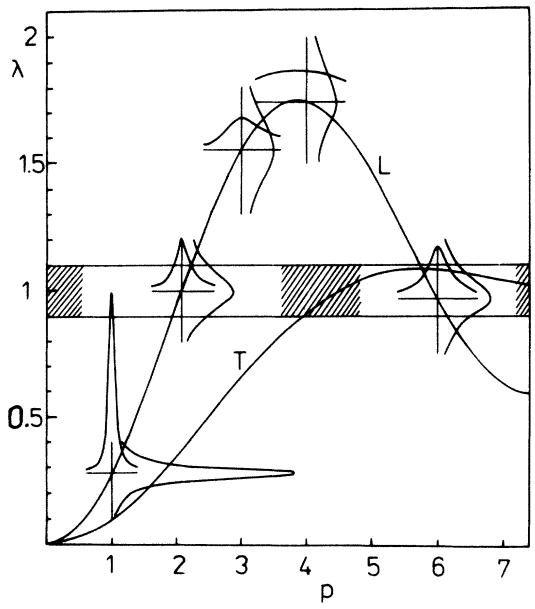

FIG. 4. Calculated NIS profiles (17) for Lorentz distribution with $a=0.1$, in several p-constant (i.e., Q-constant) and ω-constant scans. Dispersion curves (6) for purely configurational disorder, $a=0$, are also shown: here $\lambda^{\mathrm{L,T}}=3M\Omega_{\mathrm{L,T}}^2/(nl)$. Shaded area shows the $1-a<\lambda<1+a$ region.

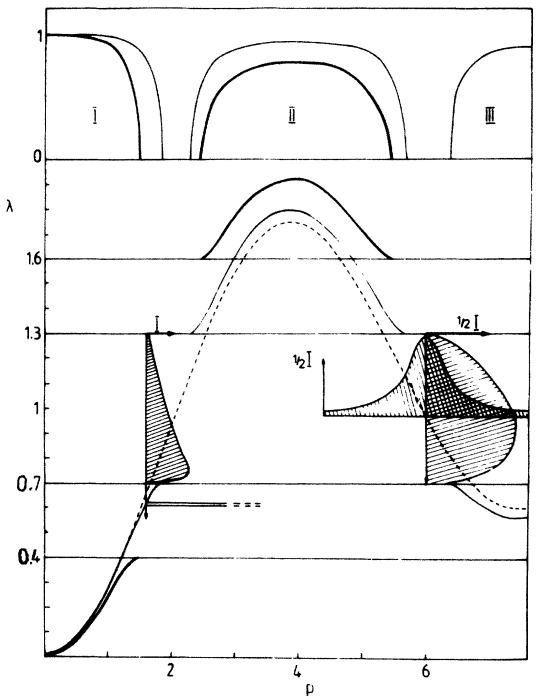

FIG. 5. Lower part: longitudinal dispersion curves for elliptic distribution. Thick line: $a=0.6$, thin line: $a=0.3$. Insets show some NIS profiles for the disorder-band parameter $a=0.3$. Horizontal lines mark the edges of the band in both cases. Dashed line is the L-dispersion curve (6) for purely configurational disorder. Upper part shows the I_p^{L} intensity [see (20)] of the δ-function part of the NIS cross section corresponding to the L-dispersion curves in lower part. Note the Q gaps and the absence of the coherence range III for $a=0.6$.

singularity at $\lambda=1.3$. Two remaining self-force distributions are smoother from it and so the number of coherence ranges is finite. Because of the continuous behavior of the function $-\lambda\Lambda_1(\lambda)$ for $\lambda\to 0$ and $f_p^{L,T}$ for $p\to 0$, there always exists the first coherence range, at least for $a<1$.

The dispersion curves $\Omega_{L,T}(p)$ given by Eq. (6), corresponding to purely configurational disorder, are also shown in Figs. 4 and 5. On comparing, we can see that force disorder (i) expands upwards the range of allowed frequencies, (ii) introduces the Q gaps, and (iii) produces broad NIS-intensity profiles in the band of disorder apart from the sharp ones outside the band.

IV. FREQUENCY SPECTRUM

Let us see in which way the force-constant disorder shows up in the frequency spectrum $g(\omega)$ or $G(\lambda)$ (total density of states). The Q summation in (2) is divergent with the ALITA Green's function—it is the main deficiency of this approximation. There is a good argument for "improving" the convergence by multiplying the Green's function with a properly chosen cutoff factor, to reduce the large-Q contribution.[3] As this step is rather arbitrary, let us first distinguish these features of the spectrum which follow directly from the details of the L and T dispersion curves and from the form of the ρ distribution of self-forces.

In the band of disorder the spectrum is just a deformed distribution $\rho(\lambda)$, as it follows from Eq. (17); see also the NIS Q-constant profiles in Fig. 5 and Sec. VII. If the band is well defined and narrow enough, we may have in the spectrum the contributions of region II and further coherence ranges. In each of them the dispersion curves attain a maximum or minimum range. These extrema contribute to the spectrum the singularities of the $x^{-1/2}$ type.[3]

If the bandwidth parameter $a<1$, then there always exists in the spectrum the Debye region, where $G\sim\lambda^{1/2}$ or $g\sim\omega^2$. The first coherence range then exists also.

Now let us do the Q integration in (2) to obtain the frequency spectrum. The Lorentz distribution of self-forces is most convenient for this purpose, because of its continuity—the band of force disorder extends indefinitely and there are no singularities. [For the convenience of calculation of the function $\Lambda_1(\lambda)$, the lower limit of integration in (14) has been shifted in this case to $-\infty$. The resulting tail of negative self-force constants $\Psi<0$ is of little importance, if the parameter a is small enough.]

The Gaussian form proposed before[3] has been used as the cutoff factor: ($p=QW$)

$$F(Q)=e^{-\alpha Q^2}\equiv e^{-(p/p_0)^2}. \tag{21}$$

To give some estimate of α or p_0, let us recall that for crystal the corresponding function may be taken as $F=1$ in the Brillouin zone, and $F=0$ besides. The volume of the zone in terms of the atomic radius r_0 is $6\pi^2/r_0^3$ (for monatomic systems). We require that with the form (21) the integral $\int Fd^3Q$ equals the same. Assuming that the distance between nearest neighbors $W\simeq 2r_0$, we obtain a fairly reasonable estimate:

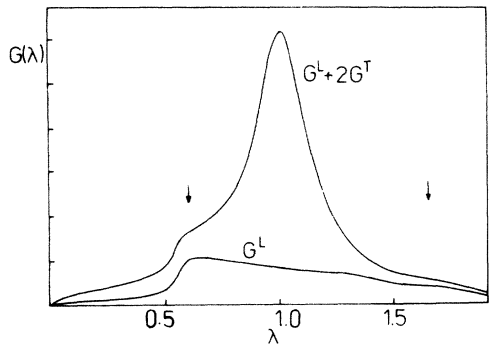

FIG. 6. Spectrum of (squared) frequencies $G(\lambda)$, Eq. (2), for the elliptic distribution of self-force constants with the disorder-band parameter $a=0.1$. Cutoff factor (21) with $p_0=6.77$ was used in the integration. The curve marked G^L shows the contribution related to the L curve in Fig. 4; the bump at $\lambda=0.6$ is a manifestation of the first minimum in the curve. Arrows show the positions of the first minimum and first maximum; for purely configurational disorder, $a=0$, the singularities of the $x^{-1/2}$ type would be present. Main peak in the full spectrum G^L+2G^T follows the behavior of the T-dispersion curve near $\lambda=1$.

$$\alpha=\frac{W^2}{4(6\pi)^{1/3}},\quad p_0=2\times 6^{1/3}\pi^{1/6}. \tag{22}$$

With the cutoff parameters near the above values, the details of the dispersion curves between $p=0$ and the second extremum may be visible in the frequency spectrum. The first minimum in the Ω_Q^L curve should show up well because the volume element of integration Q^2dQ is of great importance there and the component $[\pi\lambda\rho(\lambda)]^2$ in the denominator of (17) is relatively small. The situation is almost the opposite with the first maximum of the Ω_Q^L curve, so the corresponding contribution to the spectrum is expected to be small. The Ω_Q^T curve oscillates near $\lambda=1$. It should result in a strong peak in the spectrum near this value.

Figure 6 shows the results of such integration with the half-width $a=0.1$ and $p_0=6.77$ [larger than the estimate (22) to show the details more clearly]. They are consistent with the above predictions. Perhaps the most interesting feature is the bump about $\lambda=0.6$, corresponding to the first minimum in the Ω_Q^L, whereas the one corresponding to first minimum, about $\lambda=1.6$, is weak. Both bumps become sharper when the width parameter a decreases; besides, bumps due to other extrema in dispersion curves show up then. Qualitatively, the obtained spectrum is similar to known experimental spectra for amorphous Ge and Si,[8] as we anticipated,[2] except for the low-frequency structure in the experimental spectra.

V. DETERMINATION OF THE SPECTRUM OF EINSTEIN FREQUENCIES FROM EXPERIMENTAL DATA

A hypothetical frequency of vibration of an atom when its neighbors are frozen at their equilibrium positions is called the Einstein frequency. In a crystal there are a few

of them—e.g., for Al there is only one, $\simeq 3.8\times 10^{13}$ rad/s (Ref. 9)—and this notion is not very useful. In disordered systems the neighborhood of each atom is different from the others and so there are plenty of different Einstein frequencies. For example, the spectrum of Einstein frequencies, determined numerically by von Heimendahl[10] for a large disordered Mn-Zn cluster, shows a formidable width—about 90% of the whole squared-frequency range of the normal-mode band for this case.

In the physics of disordered solids we have too few well-conceived intrinsic characteristics. The spectrum of Einstein frequencies would certainly be of great value in this respect—it gives statistical information on the fields of force the atoms move in—on the condition that we could measure it. We show below that neutron scattering at large momentum transfers **Q** provides this function directly, at least for the present monatomic case with nearest-neighbor coupling only.

All we have to do is to put $Q\to\infty$ (i.e., $p\to\infty$) in the formula (17). In this limit $i_p\to 1$, $f_p\to\infty$, and we immediately obtain

$$\frac{d^2\sigma^{\mathrm{NIS}}}{d\omega\, d\Omega}\sim -n(\omega)\mathrm{Im}\Gamma^{\mathrm{L}}(\omega+i\varepsilon)\sim n(\omega)\rho(\lambda)\ , \tag{23}$$

i.e., from neutron inelastic scattering at large **Q** we can get the spectrum of Einstein frequencies $E(\omega)$:

$$E(\omega)=2\omega\rho\left[\frac{\omega^2}{\omega_0^2}\right]\ . \tag{24}$$

This is true for any distribution $\rho(\lambda)$ confined to a finite range of $\lambda\geq 0$. If the system is more complex, multiatomic, or if it has long-range interactions, then the formula is probably less simple, but the principle remains true. In this way, for the first time, the spectrum $E(\omega)$ has been shown to be a physical "observable."

This observation enables us to understand the interrelation between some spectra calculated numerically by Hafner[11] for the large cluster of metallic glass $Ca_{0.7}Mg_{0.3}$. He has found that at large Q several dynamical structure factors (the NIS cross section being composed of them) are "practically identical with TDOS" (total density of states), i.e., with the frequency spectrum $g(\omega)$.

In view of the result (22) they should instead be proportional to the spectrum of Einstein frequencies, $\rho(\lambda)$ or $E(\omega)$. As mentioned in Sec. IV, in the band of disorder the squared-frequency spectrum $G(\lambda)$ is the ρ distribution, properly deformed, and a similar relation holds between the functions $g(\omega)$ and $E(\omega)$. When both spectra are spread over the same frequency range, then they can be close to each other, which explains the Hafner result.

At the same time we have to emphasize that in spite of all possible similarities the dynamical structure factor at large **Q** [i.e., the function $E(\omega)$] and the frequency spectrum $g(\omega)$ are basically different in their physical content. This fact follows directly from our simple and transparent formulation, but seems to have been obscured somewhat in numerical procedure.

VI. ON THE NATURE OF NORMAL MODES OF VIBRATION IN DISORDERED SOLIDS

A neutron probe may be represented by a plane wave (PW). It is able to interfere with the PW components of normal modes of vibration and thus give us information on them. The result of such PW testing is contained in the function $\langle\overleftrightarrow{G}_Q(\omega)\rangle$. In the present case the following conclusions may be drawn.

No plane-wave deformations with wave vectors from the Q gaps can be present in the normal modes. In contrast, the deformations with Q belonging to the coherence ranges can participate in the modes. Qualitatively, the amplitude I_p is a measure of such participation—we can see in Fig. 5 how rapidly I_p falls to zero when the corresponding Q approaches the Q gap.

At long wavelengths $Q\to 0$, one knows *a priori* that the PW deformations are the normal modes in disordered solids—this is a continuum limit and atomicity plays no role. On the other hand, one expects that just the discrete nature of the system should inhibit the propagation of too short waves. In the present model one indeed finds that the dispersion curve in the first coherence range ends up on $p=1.8$ (for $a=0.3$, see Fig. 5), corresponding to the wavelength $\simeq 3.5W$. But, rather unexpectedly, we arrive at coherence ranges at still shorter wavelengths. The second one is centered roughly at $p=4$ and provides the highest-frequency PW component of normal modes in the system. The appearance of the second and further coherence ranges depends on the shape and width of the ρ distribution. It is the force-disorder that creates the Q gaps—in the case of purely configurational disorder the coherence range is infinite.

Let us look at the Q-constant NIS profile in Fig. 5 for $p=1.6$, $a=0.3$. It consists of the $\delta(\lambda-\lambda_p^{\mathrm{L}})$-type peak at $\lambda=0.61$ with the intensity factor $I=0.78$, and a broad profile through the whole self-force disorder band. Although confined to the band, the profile is different from the original elliptic ρ distribution [as is obvious from (17)], and its shape depends on Q through f_p^{L} (16). When the dispersion curve approaches the band, the intensity I_p^{L} falls to zero, whereas the total in-band intensity increases, its peak approaching the band edge. The ω-constant NIS intensity, according to (17), never reaches zero in the band.

To fully exploit the meaning of the above, let us figure out the system of decoupled atoms vibrating with single Einstein frequency ω_0:

$$-\mathrm{Im}\langle\overleftrightarrow{G}_Q(\omega+i\varepsilon)\rangle\sim -\mathrm{Im}\langle L\rangle\sim\delta(\omega-\omega_0)\ .$$

In the Q-constant NIS scan a perfect PW normal mode (if there was one) and the PW component of localized vibration would show up as similar narrow peaks. The situation changes drastically in the ω-constant scan: the plane-wave normal mode again provides a narrow peak, whereas the local mode provides a constant intensity of scattered neutrons at the energy transfer $\hbar\omega=\hbar\omega_0$, zero otherwise. If instead of the single level ω_0 there is a band of disorder, then, in the same scan, the intensity may vary a little instead of being constant [see Eq. (17)], but narrow

δ-function-like peaks are still to be expected only beside the band. The situation remains qualitatively the same if we switch on the coupling between the atoms, except that now the intensity in the band is lower—part of the degrees of freedom have been used to set up the plane-wave components of normal modes. The ω-constant scan is therefore appropriate for identification of the band of disorder which, in a sense, is also the band of frequencies of localized modes.

One should emphasize here, however, that our distinction between localized modes and those involving plane waves does not have a direct relevance to the Anderson localization concepts. There, one seeks conditions under which a given atom can vibrate with a single definite frequency.[12] Here, one investigates the whole macroscopic system for the plane-wave contamination of its normal modes of vibration.

VII. ACOUSTIC LIMIT

The low-temperature "vibrational" specific heat C_V of some disordered three-dimensional systems shows the T^n behavior with $n<3$. As at low frequencies the frequency spectrum $g\sim\omega^{n-1}$, this means that in such solids there is a deviation from the typical Debye behavior $g\sim\omega^2$. Hence there must be a deviation from the linear relation between the normal-mode frequency ω and wave vector q, $\omega\sim q$, at long wavelengths.

Just in this limit is it reasonable to identify the NIS dispersion curves discussed in this paper with the dispersion curves of vibrational modes in the solid. Let us therefore see whether the force disorder may modify the usual ω versus q dependence.

It can happen only when the force-disorder band [i.e., the λ range where $\rho(\lambda)\neq 0$] reaches the $\lambda=0$ point, i.e., for $a=1$. Details of the edge of the ρ-distribution at $\lambda\to 0$ are essential here. Elliptic distribution and, with some reservation, Lorentz distribution, lead to the usual $\omega\sim q$, because $\Lambda_1(\lambda)\to$const as $\lambda\to 0$. With rectangular distribution, in the limit $\lambda\to 0$, $q\to 0$, Eq. (19) gives

$$-\omega^2\ln\omega\sim q^2 ,$$

$$g(\omega)\sim\omega^2(-\ln\omega)^{3/2}$$

and

$$C_V\sim T^3(-\ln T)^{3/2} ,$$

which is a definite modification of the Debye behavior. It is easy to check that with $\Lambda_1(\lambda)\to-\lambda^{-1/3}$ as $\lambda\to 0$, we would have $g(\omega)\sim\omega$, which leads to $C_V\sim T^2$, whereas with $\Lambda_1(\lambda)\to-\lambda^{-2/3}$ as $\lambda\to 0$ there is $g(\omega)\sim$const, which leads to $C_V\sim T$. The form of the corresponding functions $\rho(\lambda)$ is not known, but obviously they must be singular at the zero frequency edge. This means there is a strong accumulation of self-force constants (or Einstein frequencies) approaching zero. It makes the system unstable with respect to macroscopic deformations. In the present nearest-neighbor central-force model this is the only way to make the system "floppy" in the sense of Phillips and Thorpe.[13] With a more flexible model, e.g., one such as the axial force model, one may possibly arrive at instabilities also at short wavelengths, on allowing the first minimum in the ω_Q^L curve to approach zero. Some such effects appear when $t/l\simeq-0.2$, where t represents the isotropic coupling in the above-mentioned model.[3]

VIII. CONCLUSIONS

The influence of the force-constant disorder on dynamical characteristics of disordered solids has been calculated exactly, within the ALITA, for the nearest-neighbor central-force model of interatomic coupling. The force disorder manifests itself in the smoothing of the details of the frequency spectrum, as compared to the one for purely configurational disorder, in the appearance of the Q gaps in dispersion curves for such plane-wave deformations which cannot be components of normal modes of vibration, and in the possibility of essential deviation from the T^3 law for the specific heat of the three-dimensional disordered solids at $T\to 0$. Neutron inelastic scattering at large momentum transfer has been shown to provide the spectrum of Einstein frequencies, which in this way becomes physically observable. Numerical data of other authors show that this spectrum can spread over a wide range of frequencies. It should be considered as one of basic characteristics of disordered solids. Possibly, to be successful in understanding the dynamics of such systems in more complex cases, one should first determine and then take into account this characteristic. In general, it can be done within the ALITA.

The present approximation exaggerates the importance of the poles of the locator and, for many **Q** vectors, does not provide any broadening. Usually the broadening of the modes enters into theories via single-site multiple scattering—see, e.g., the papers of Roth[14] and Singh[15] on electronic structure of amorphous systems. In the present work the broadening appears, for frequencies in the band of disorder, as a manifestation of finite width of the spectrum of self-forces. No broadening appears for the frequencies outside the band, which is a deficiency of the approximation.

Nevertheless, there is evidence[10,11] that for some systems the band of disorder covers a great part of the frequency range where $g(\omega)\neq 0$. In such cases traditional efforts aimed at incorporating all multiple-scattering contributions into theory may turn out to be less practical than taking into account the correct width and shape of the Einstein frequency spectrum $E(\omega)$.

ACKNOWLEDGMENT

The author is grateful to Professor A. Holas, Professor J. Hafner, and Professor H. Krumbhaar-Müller for valuable discussions.

[1]J. Hafner, in *Glassy Metals I,* Vol. 46 of *Topics in Applied Physics,* edited by H. Beck and H. J. Gutherodt (Springer, Berlin, 1981).
[2]A. Czachor, Phys. Rev. B **32**, 5628 (1985).
[3]A. Czachor, Acta Phys. Pol. A **69**, 281 (1986).
[4]A. B. Bhatia and R. N. Singh, Phys. Rev. B **31**, 4751 (1985).
[5]A. Zinken, U. Buchenau, H. Fenzl, and H. Schober, Solid State Commun. **22**, 693 (1977).
[6]W. A. Kamitakahara and J. R. Copley, Phys. Rev. B **18**, 3772 (1978).
[7]N. Kunimoti, Y. Tsunoda, N. Wakabayashi, R. M. Nicklow, and H. G. Smith, Solid State Commun. **25**, 921 (1978).
[8]R. Alben, D. Weaire, J. E. Smith, and M. H. Brodsky, Phys. Rev. B **11**, 2271 (1975).
[9]A. Czachor, *Atomic Vibrations in Solids* (Polish Scientific Publishers, Warsaw, 1982) (in Polish).
[10]L. von Heimendahl, J. Phys. F **9**, 161 (1979).
[11]J. Hafner, Phys. Rev. B **27**, 678 (1983).
[12]J. M. Ziman, *Models of Disorder* (Cambridge University Press, Cambridge, England, 1979).
[13]J. C. Phillips and M. F. Thorpe, Solid State Commun. **53**, 699 (1985).
[14]L. M. Roth, Phys. Rev. B **9**, 2476 (1979).
[15]V. J. Singh, Phys. Rev. B **24**, 4852 (1981).